New Ways of Looking at Simulation Output

B. W. Bush

5 September 1996

Outline

Preliminaries

Rényi Entropy

Multiresolution Analysis

Scaling Behavior

Prospects

The CA Grid

The layout of the cellular automaton grid is shown in Figure 1.

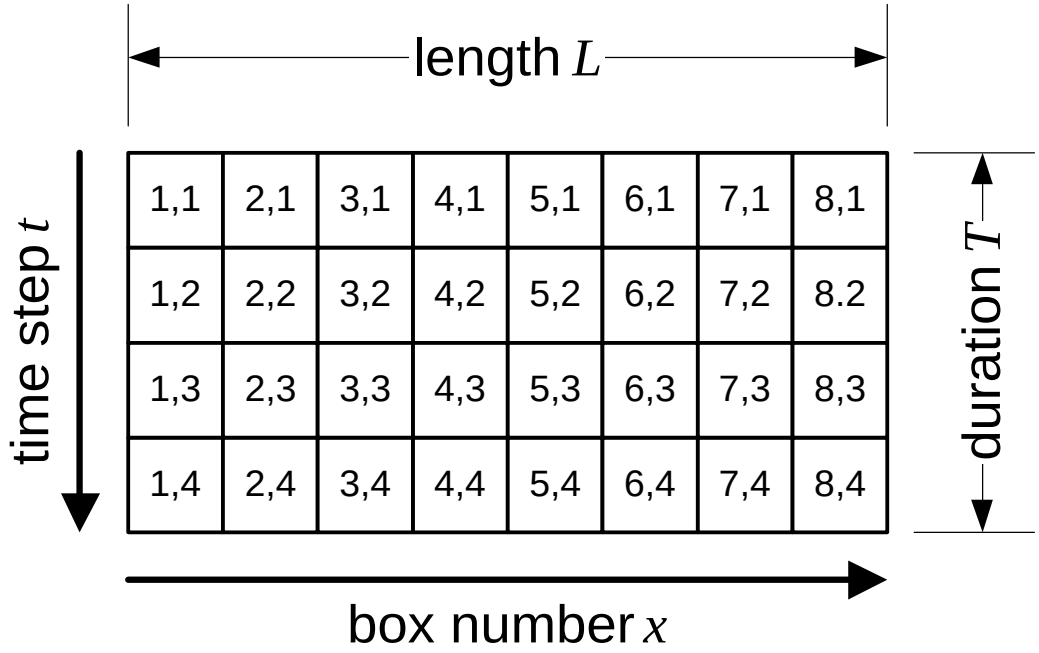

Figure 1. The coordinate system used for the cellular automaton grid.

The CA Grid (continued)

Here we consider only single lane driving on a road with periodic boundary conditions. Each cell may contain at most one vehicle. The *velocity* of the cell (x,t) is written $v_{x,t}$ and is subject to the constraints

(1) $$v_{x,t} \in \{0,1,\ldots,v_{\max}\},$$

where $v_{\max}$ is the speed limit. Of course, the velocity $v_{x,t}$ is only defined when there is a vehicle present at the cell (x,t).

Driving Rules

Let $g_i(t)$ be the *gap* (the number of empty cells) in front of vehicle i, whose position and velocity at time t are $x_i(t)$ and $v_i(t)$, respectively. The evolution of the CA is given by

(2) $$x_i(t+1) = x_i(t) + v_i(t+1)$$

and

(3) $$v_i(t+1) = \max\left[0, \min\left\{v_i(t)+1, g_i(t), v_{\max}\right\} - R\right]$$

where R is an independent random variable with

(4) $$\mathrm{P}(R=1) = p_{\mathrm{decel}} \text{ and } \mathrm{P}(R=0) = 1 - p_{\mathrm{decel}},$$

so p_{decel} is the probability of decelerating. Here we take $p_{\mathrm{decel}} = 0.3$ throughout.

Driving Rules (continued)

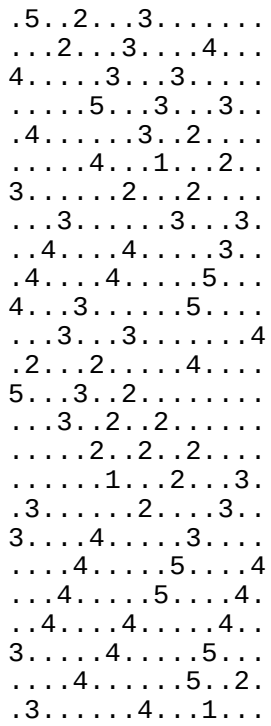

Figure 2. Example time evolution of a traffic cellular automaton with three vehicles and a grid of sixteen cells.

Labeling States

Each cell in the CA has $k = v_{\max} + 2$ possible values. We label each single-cell configuration by an integer,

(5) $$c_{x,t} = \begin{cases} v_{x,t} + 1 & \text{if there is a vehicle at } (x,t) \\ 0 & \text{otherwise} \end{cases} .$$

We also label a configuration $\{c\}$ of length L and duration T by an integer $j \in \{1,2,\ldots,k^{XT}\}$,

(6) $$j(\{c\}) = 1 + \sum_{t=1}^{T} \sum_{x=1}^{L} c_{x,t} \, k^{(t-1)L+x-1} .$$

This scheme of labeling states does not take account of the distinguishability of vehicles.

Escort Distribution

Let p_j be the probability of observing the state j in a sample of length L and duration T. We use the method of *escort distributions* to probe the structure of this probability distribution. The *escort probabilities* associated with the p_j are

$$P_j = \exp\left[\beta(F_\beta - b_j)\right] = \frac{(p_j)^\beta}{\sum_{i=1}^{k^{XT}} (p_i)^\beta} . \tag{7}$$

and we define the *bit number* for the state $_j$ as

$$b_j = -\ln p_j , \tag{8}$$

so we can write

$$p_j = \exp(-b_j) . \tag{9}$$

Helmholz Free Energy

The *partition function* and *Helmholtz free energy* at an inverse "temperature" β are

(10) $$Z_\beta(X,T) = \sum_{j=1}^{k^{XT}} \exp(-\beta b_j) = \sum_{j=1}^{k^{XT}} (p_j)^\beta$$

and

(11) $$F_\beta(X,T) = -\beta^{-1} \ln Z_\beta(X,T) ,$$

respectively. Here the bit number plays the role of then "energy" of the state. For $\beta = 1$, the escort probability is identical to the probability; other interesting cases are $\beta = 0$ (all states have equal probability), $\beta \to +\infty$ (the largest probability dominates), and $\beta \to -\infty$ (the smallest probability dominates).

Rényi Entropy

The Rényi entropy is written

(12) $$S_\beta(X,T) = \frac{\beta}{1-\beta} F_\beta(X,T) = \frac{1}{1-\beta} \ln \sum_{j=1}^{k^{XT}} (p_j)^\beta \ .$$

It can be considered as the “free information” of the system.

Special Cases of Rényi Entropy

Special cases are the *set entropy*

(13) $$S_0(X,T) = \lim_{\beta \to 0} S_\beta(X,T) = \ln \sum_{j=1}^{k^{XT}} \theta(p_j) ,$$

the *measure entropy* (or *Shannon entropy*)

(14) $$S_1(X,T) = \lim_{\beta \to 1} S_\beta(X,T) = -\sum_{j=1}^{k^{XT}} p_j \ln p_j ,$$

and the *correlation entropy*

(15) $$S_2(X,T) = -\ln \sum_{j=1}^{k^{XT}} (p_j)^2 .$$

Here we have introduced a function: $\theta(x) = \begin{cases} 1 & \text{for } x > 0 \\ 0 & \text{otherwise} \end{cases}$.

Dimension

It is also useful to define a *reduced entropy*

(16) $$s_\beta(X,T) = \frac{S_\beta(X,T)}{\ln k^{XT}}$$

and a *dimension*

(17a) $$d_\beta^X(T) = \lim_{X\to\infty} s_\beta(X,T)\,,$$

(17b) $$d_\beta^T(X) = \lim_{T\to\infty} s_\beta(X,T)\,,$$

(17c) $$d_\beta^{XT} = \lim_{X,T\to\infty} s_\beta(X,T)\,.$$

These concepts have been applied previously to deterministic cellular automata. For a multifractal we have $0 < d_\beta < 1$.

Properties of Rényi Entropy

The Rényi entropy obeys a subadditivity condition

(18a) $$S_\beta(X_1,T)+S_\beta(X_2,T)\geq S_\beta(X_1+X_2,T),$$

(18b) $$S_\beta(X,T_1)+S_\beta(X,T_2)\geq S_\beta(X,T_1+T_2),$$

where equality holds if and only if the two blocks being added are uncorrelated.

The reduced Rényi entropy also obeys several interesting inequalities:

(19a) $$0\leq s_\beta(X,T)\leq 1,$$

(19b) $$s_\beta(X,T)\leq s_{\beta'}(X,T) \text{ for } \beta>\beta'$$

Properties of Dimension

Corresponding inequalities for the dimension are

(20a) $$0 \le d_\beta \le 1 ,$$

(20b) $$d_\beta \le d_{\beta'} \text{ for } \beta > \beta' ,$$

(20c) $$d_{\beta'} \ge \frac{\beta'}{\beta'-1}\frac{\beta-1}{\beta} d_\beta \text{ for } \beta' > \beta > 1 \text{ or } 0 > \beta' > \beta .$$

Limits on the Entropy

The conservation of vehicles puts another limit on the entropy. Since the number of possible states with n vehicles is

(21) $$N_n(X,T) = (k-1)^n \binom{XT}{n},$$

the set entropy is limited by

(22) $$s_0(X,T) \le \frac{n\ln(k-1) + \ln\binom{XT}{n}}{XT\ln k}.$$

More stringent limits on the set entropy can be obtained by enumerating "legal" configurations (i.e., configurations reachable by evolving from other legal configurations) of the cellular automaton.

Numerical Experiments

This section presents results of a variety of numerical experiments on single-lane traffic cellular automata. The measurements are started after enough time steps have passed for the dependence on the initial conditions to be lost.

Measuring the Rényi entropy is difficult because the large number possible configurations $N_n(X,T)$ requires extensive sampling of the cellular automaton to obtain reasonable estimates of the state probabilities p_j.

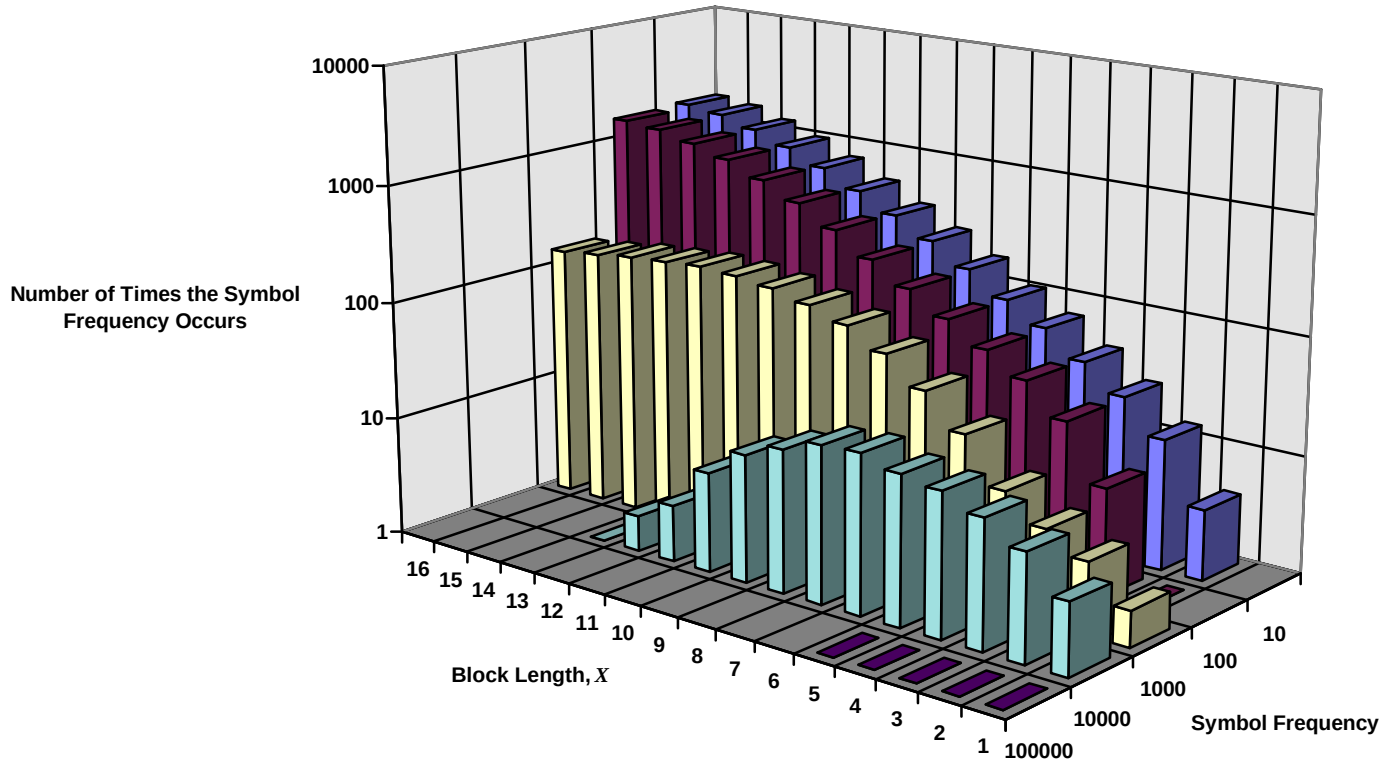

Figure 3. Experimental distribution of symbol frequency (number of times a given symbol j appears) for a variety of block length X in 80,000 samples of a sixteen-cell CA with periodic boundary conditions and three vehicles.

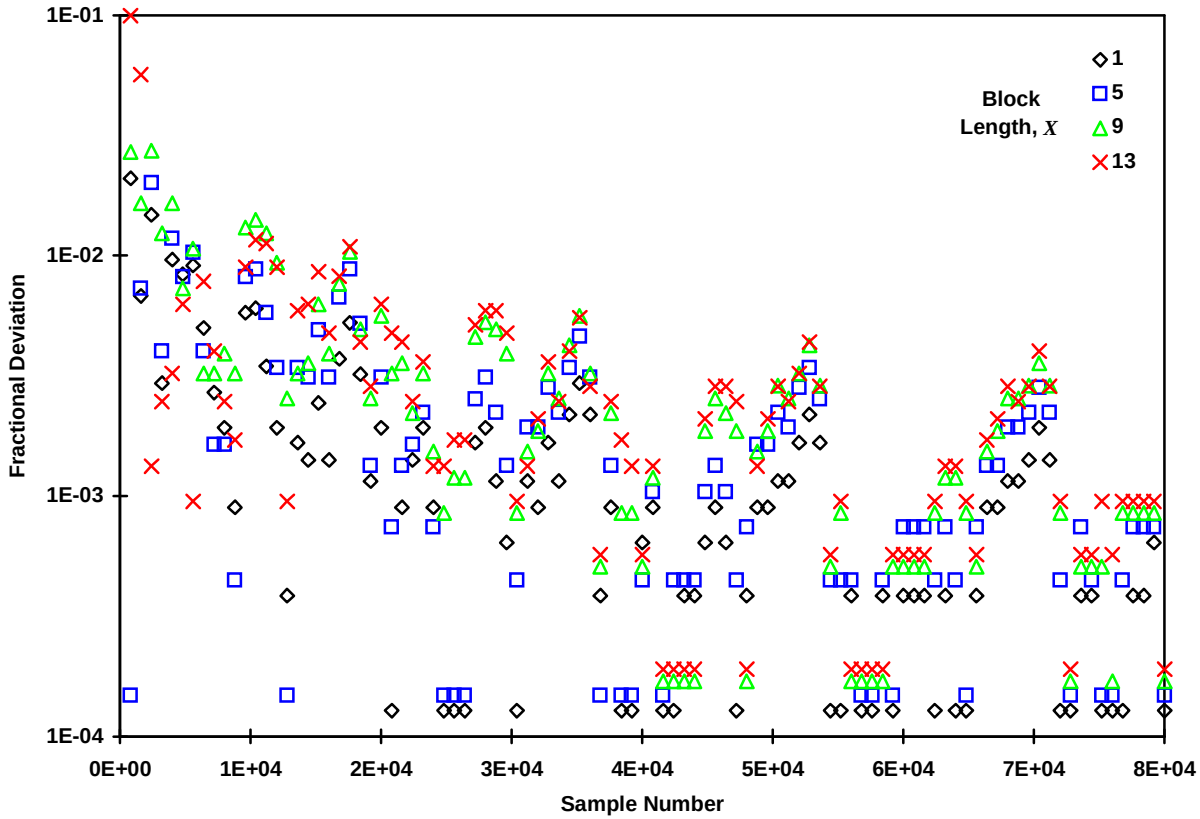

Figure 4. Experimental deviation of measure entropy $s_1(X,1)$ from its value at 80,000 samples for a variety of block length X in a sixteen-cell CA with periodic boundary conditions and three vehicles.

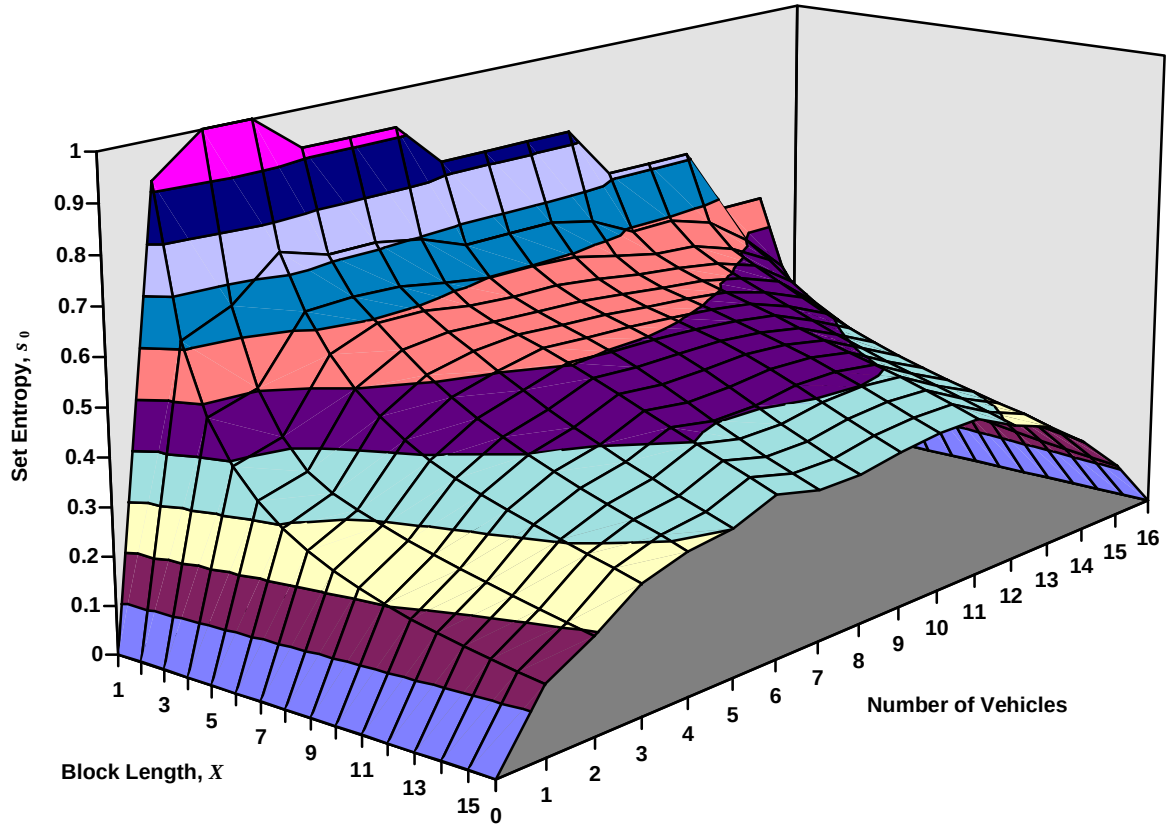

Figure 5a. Experimental dependence of set entropy $s_0(X,1)$ on block length X and number of vehicles in 80,000 samples of a sixteen-cell CA with periodic boundary conditions.

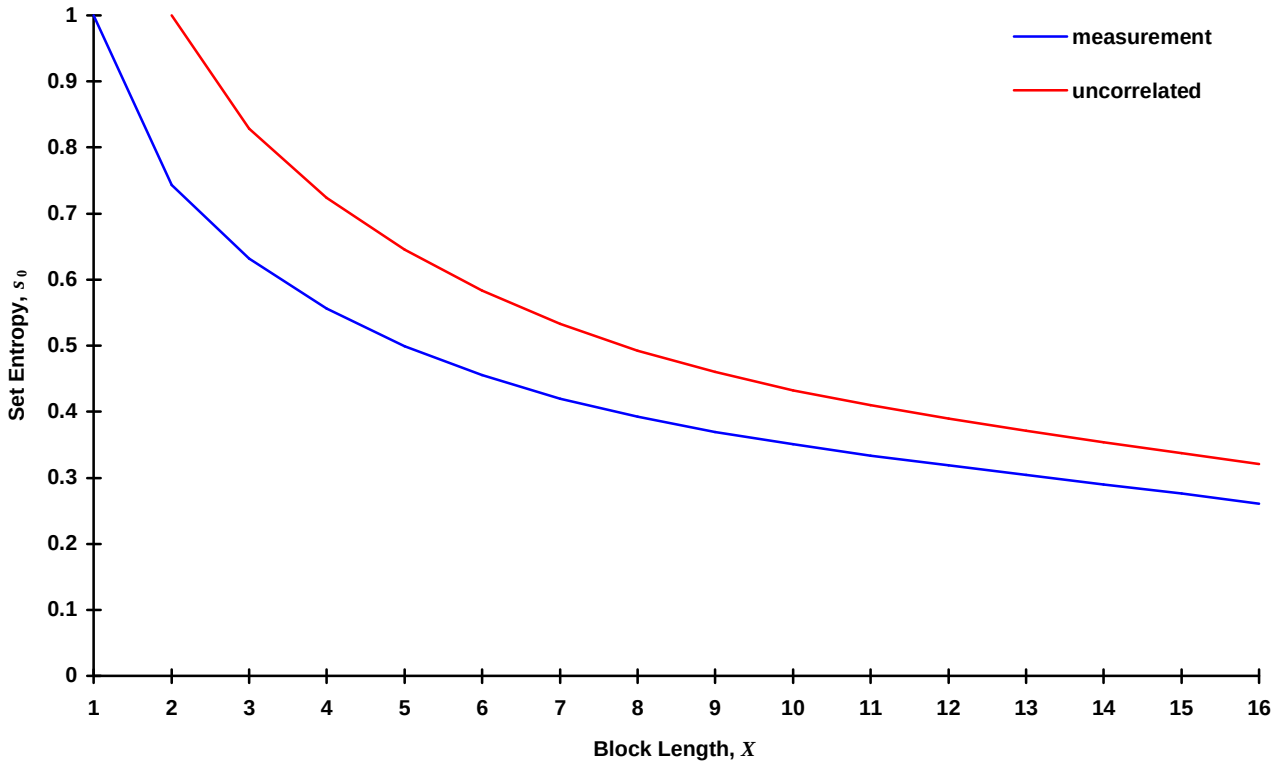

Figure 5b. Experimental dependence of set entropy $s_0(X,1)$ on block length X for three vehicles in 80,000 samples of a sixteen-cell CA with periodic boundary conditions; the red line indicates the limit given by Equation (18a).

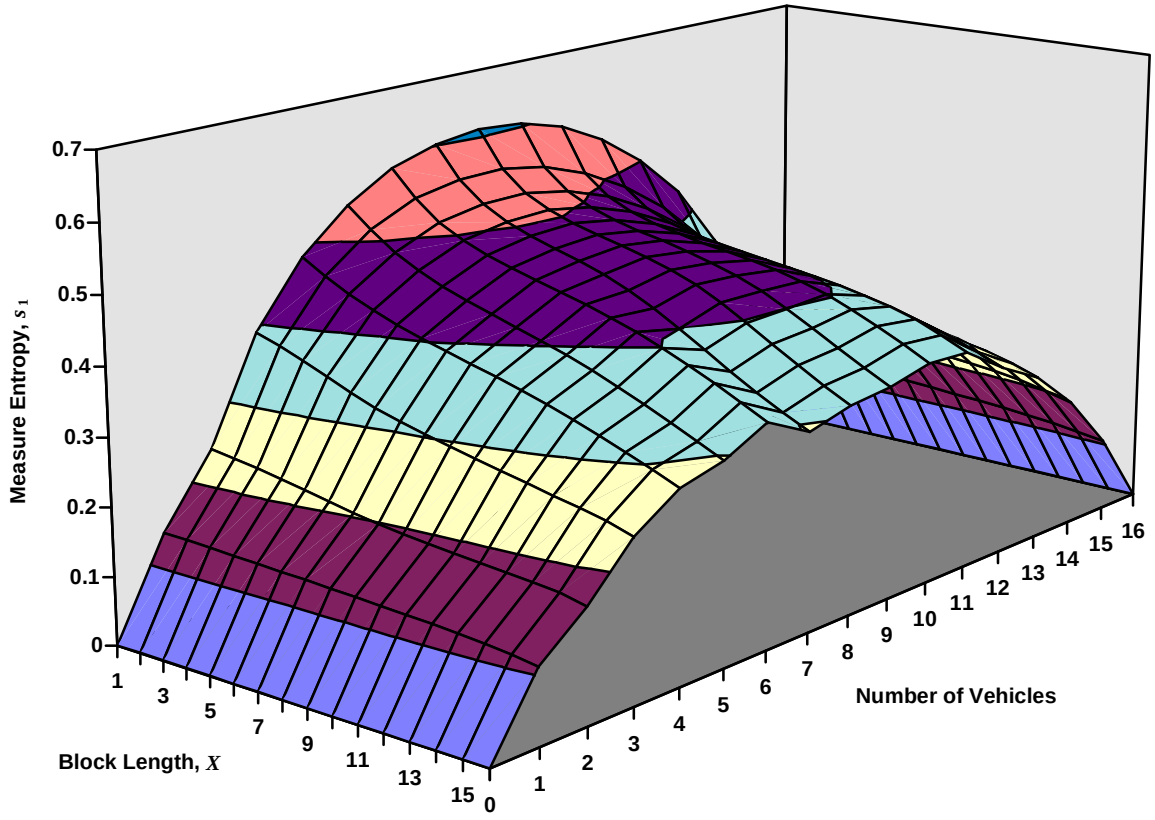

Figure 6a. Experimental dependence of measure entropy $s_1(X,1)$ on block length X and number of vehicles in 80,000 samples of a sixteen-cell CA with periodic boundary conditions.

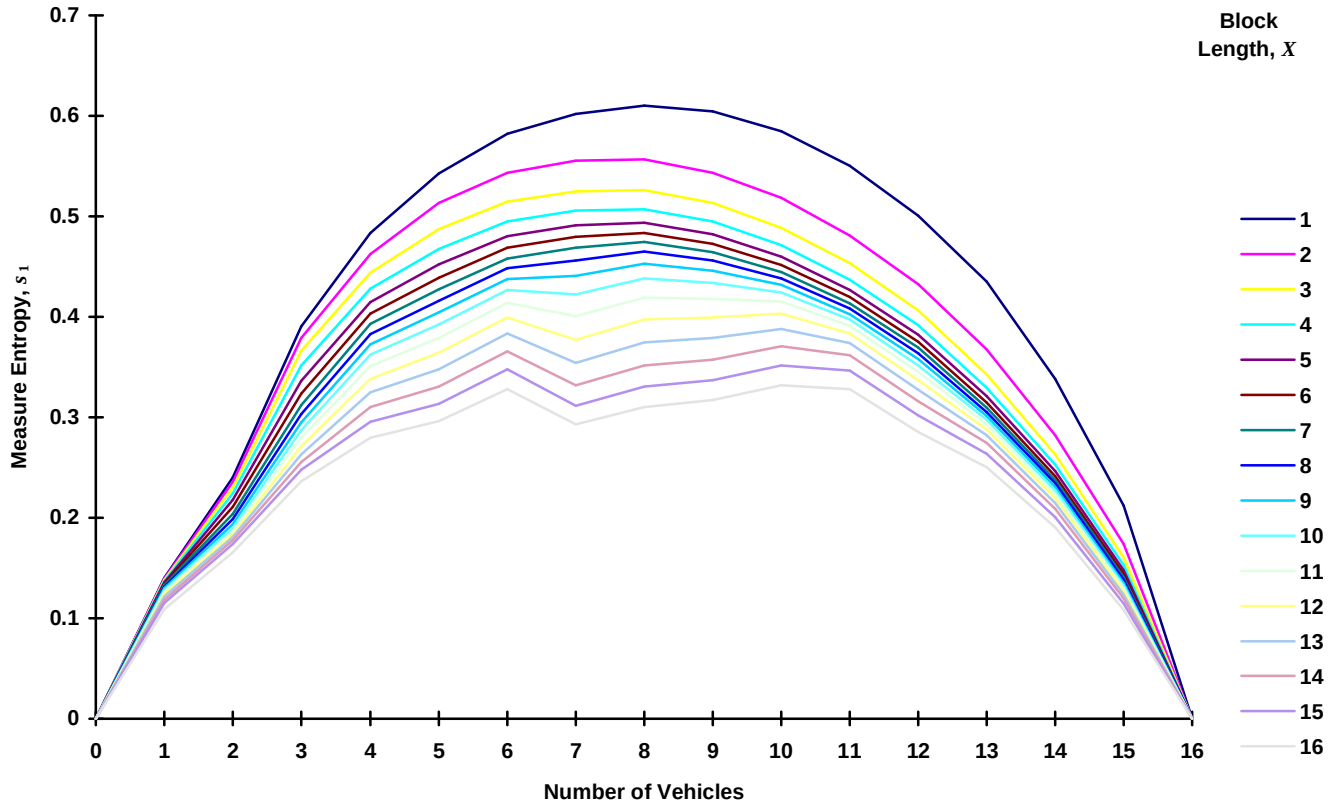

Figure 6b. Experimental dependence of measure entropy $s_1(X,1)$ on number of vehicles for a variety of block lengths X in 80,000 samples of a sixteen-cell CA with periodic boundary conditions.

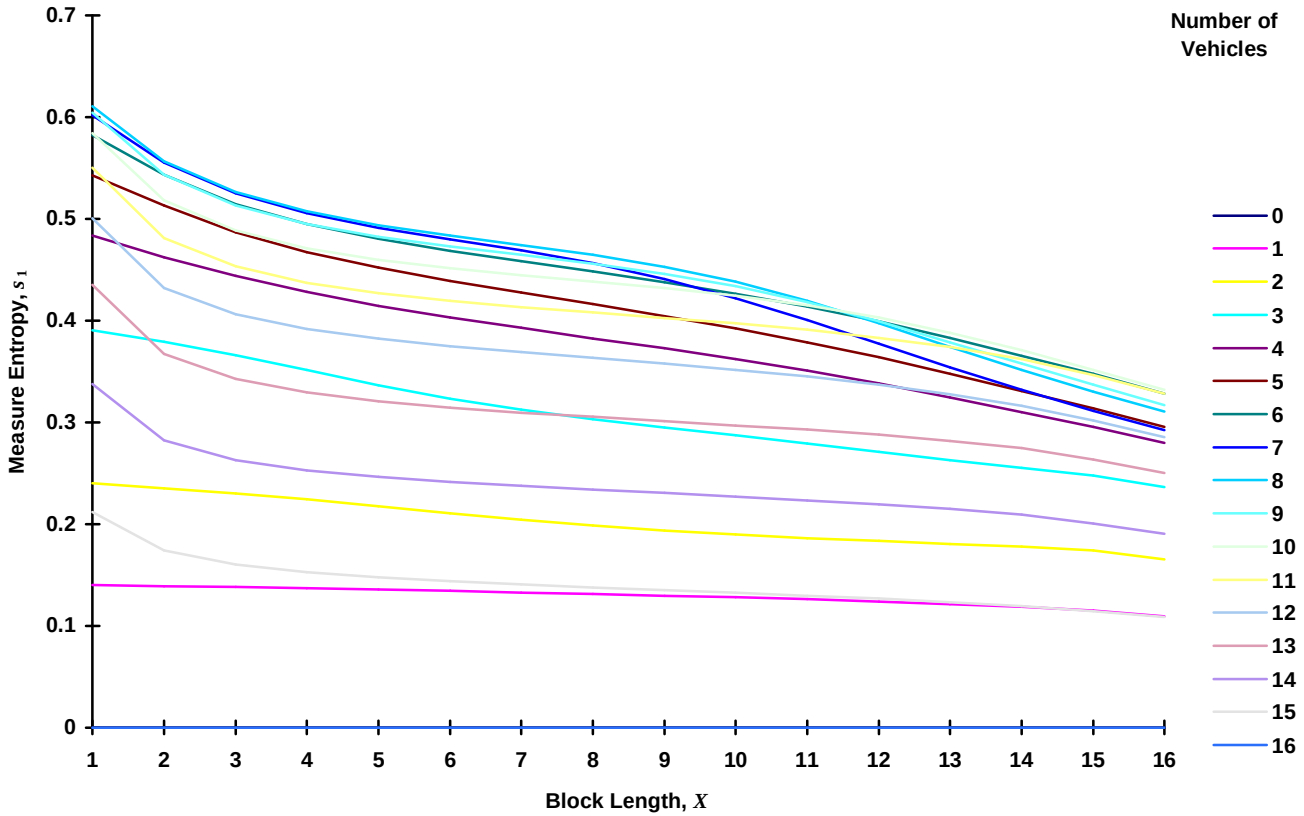

Figure 6c. Experimental dependence of measure entropy $s_1(X,1)$ on block size X for a variety of vehicle numbers in 80,000 samples of a sixteen-cell CA with periodic boundary conditions.

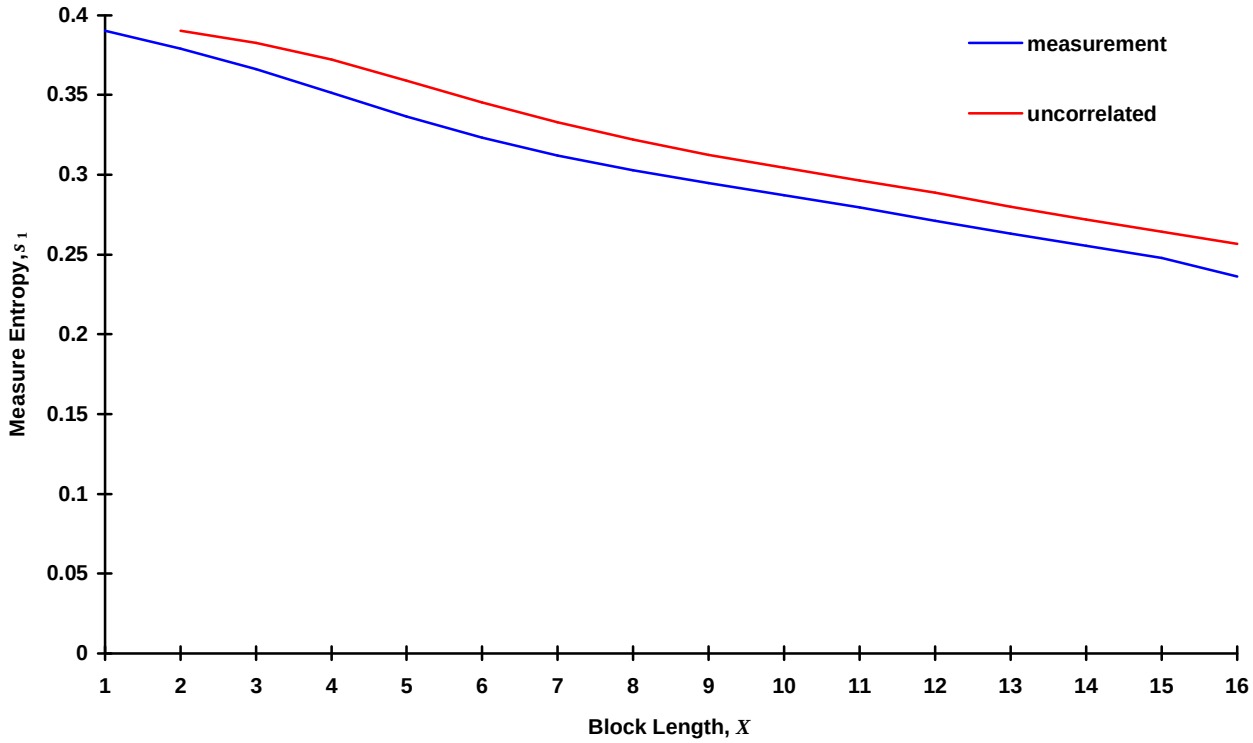

Figure 6d. Experimental dependence of measure entropy $s_1(X,1)$ on block size X for three vehicles in 80,000 samples of a sixteen-cell CA with periodic boundary conditions; the red line indicates the limit given by Equation (18a).

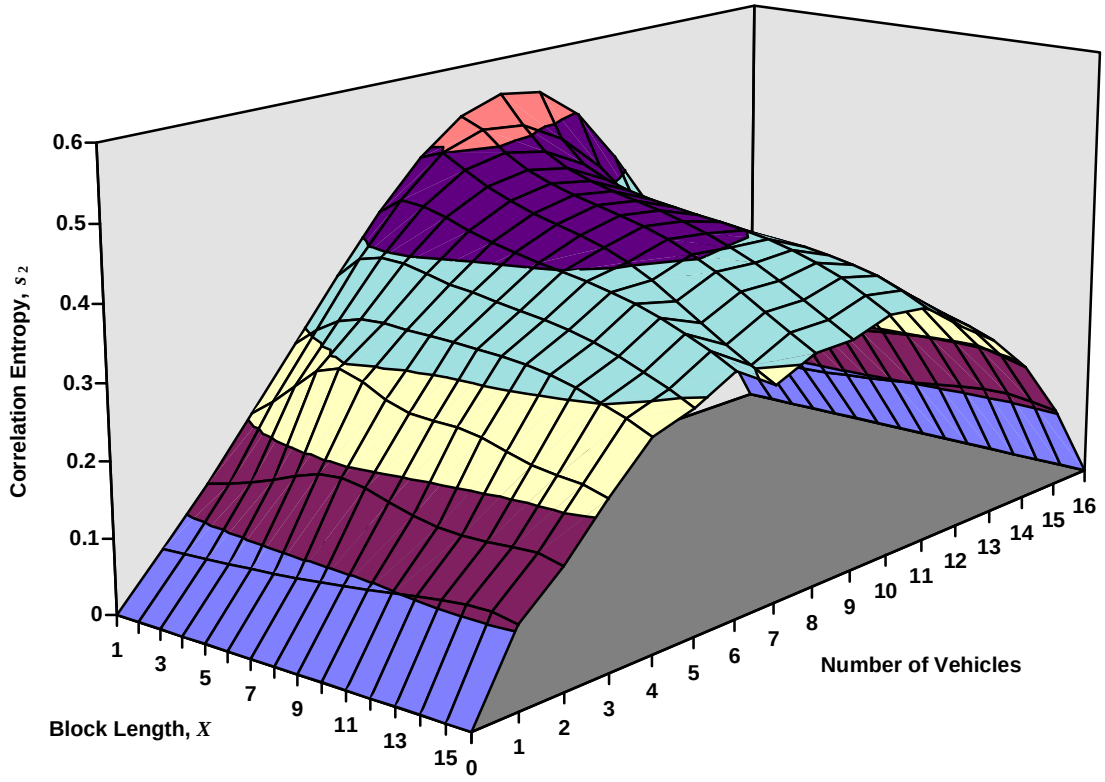

Figure 7. Experimental dependence of correlation entropy $s_2(X,1)$ on block length X and number of vehicles in 80,000 samples of a sixteen-cell CA with periodic boundary conditions.

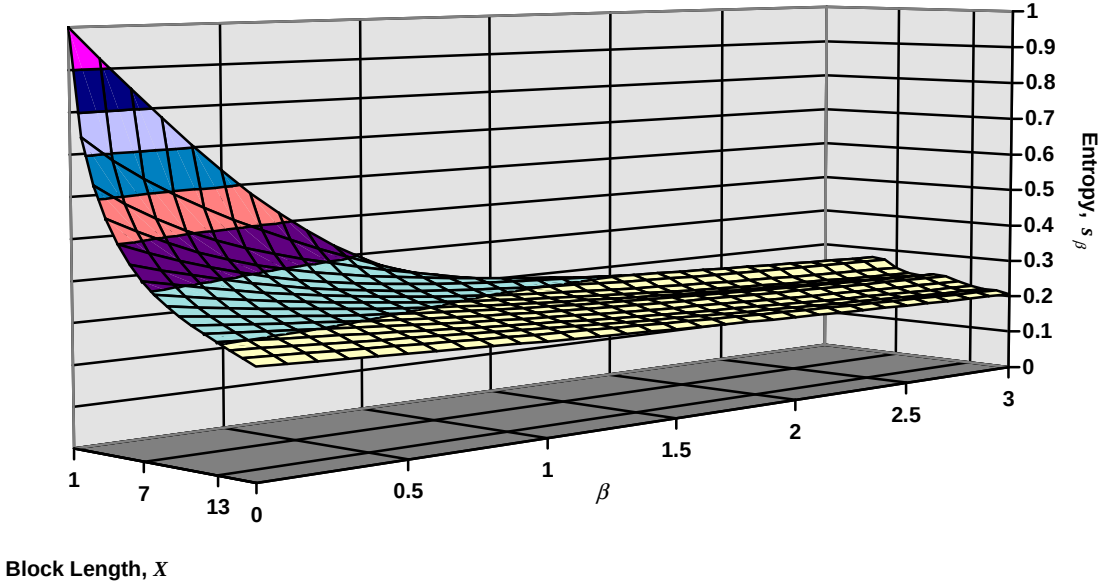

Figure 8. Experimental dependence of entropy $s_\beta(X,1)$ on block length X and number of vehicles in 80,000 samples of a sixteen-cell CA with periodic boundary conditions and having three vehicles.

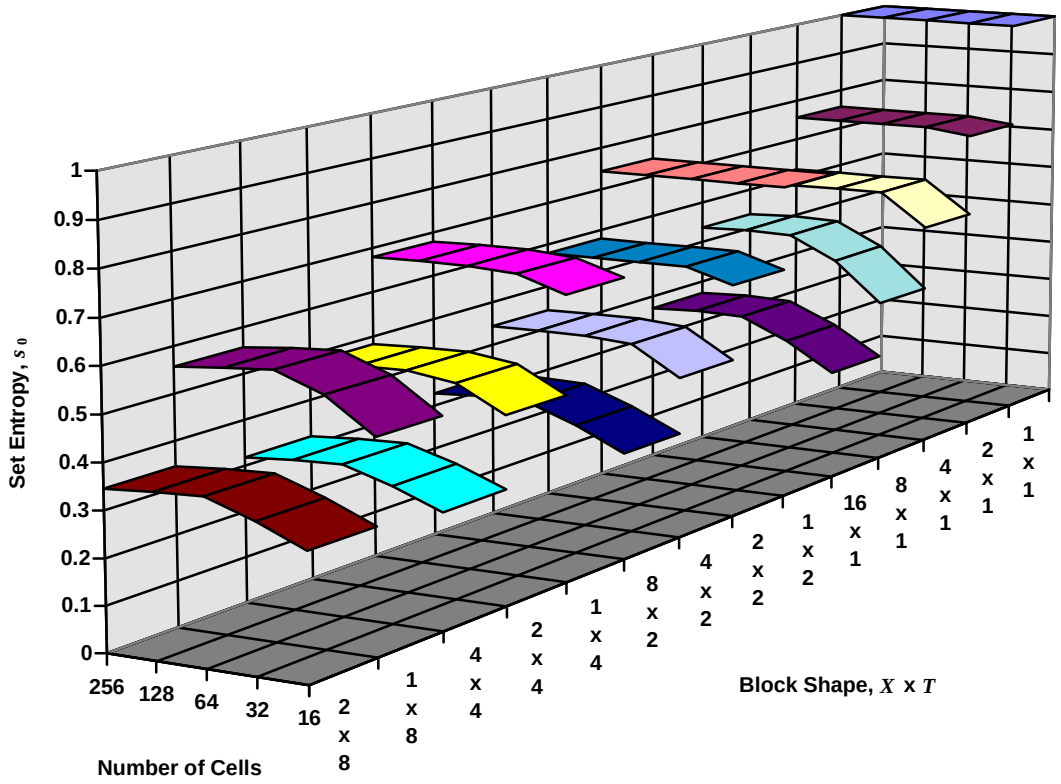

Figure 9a. Experimental dependence of set entropy $s_0(X,T)$ on block length X and duration T as a function of number of cells in 76,800 samples of a CA with periodic boundary conditions and having a vehicle density of 3/16.

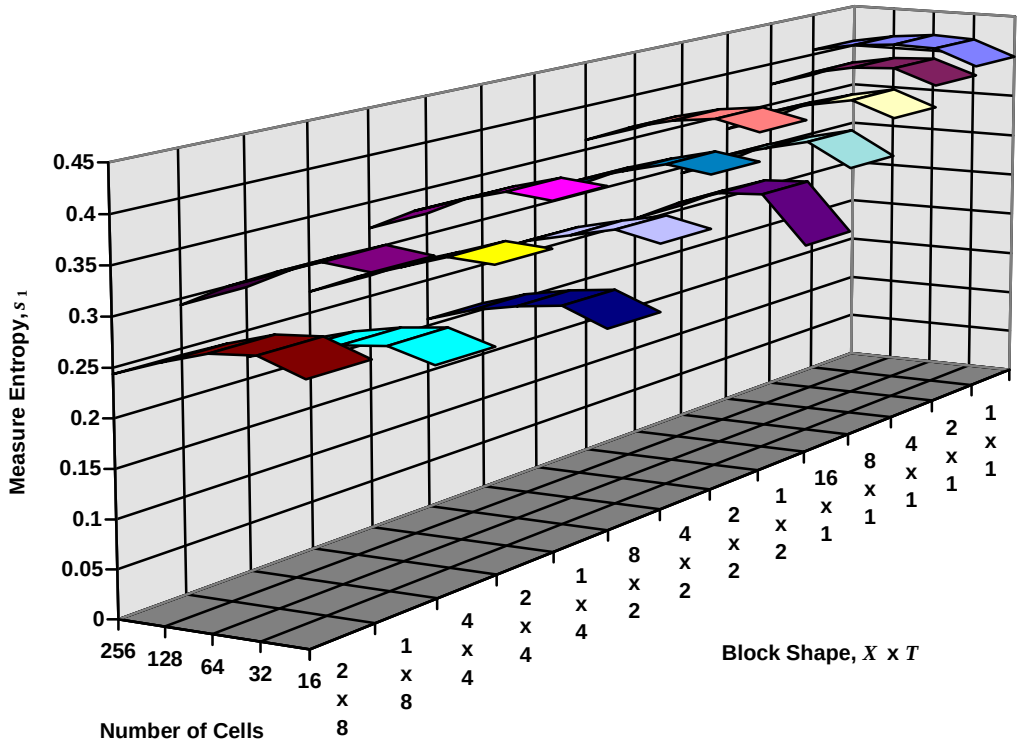

Figure 9b. Experimental dependence of measure entropy $s_1(X,T)$ on block length X and duration T as a function of number of cells in 76,800 samples of a CA with periodic boundary conditions and having a vehicle density of 3/16.

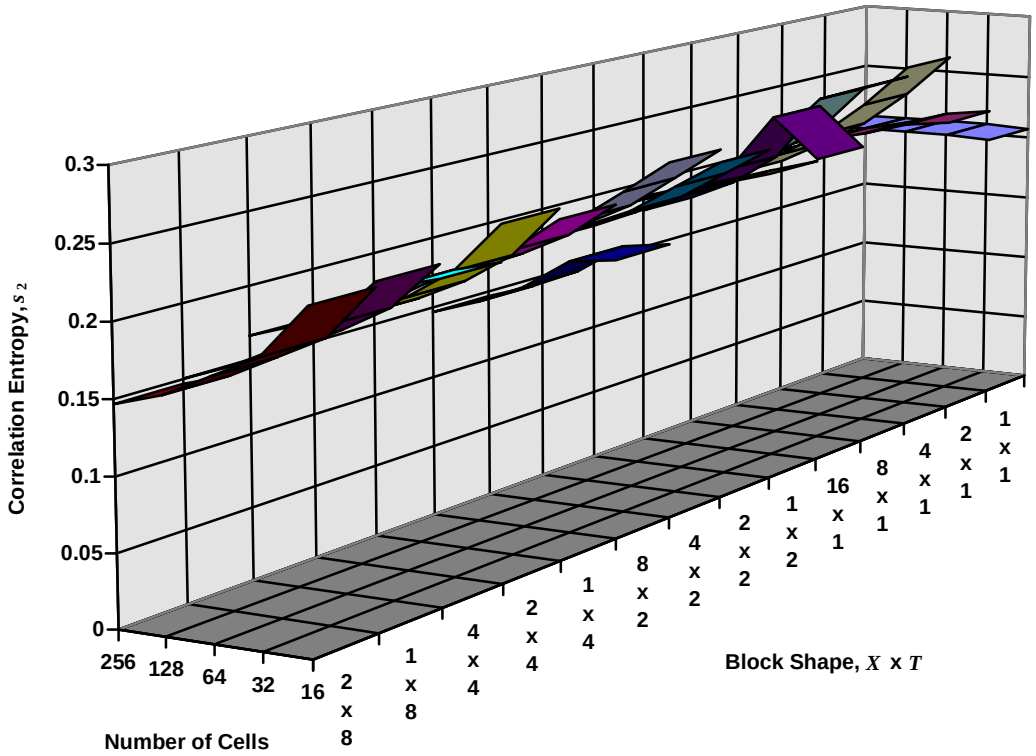

Figure 9c. Experimental dependence of correlation entropy $s_2(X,T)$ on block length X and duration T as a function of number of cells in 76,800 samples of a CA with periodic boundary conditions and having a vehicle density of 3/16.

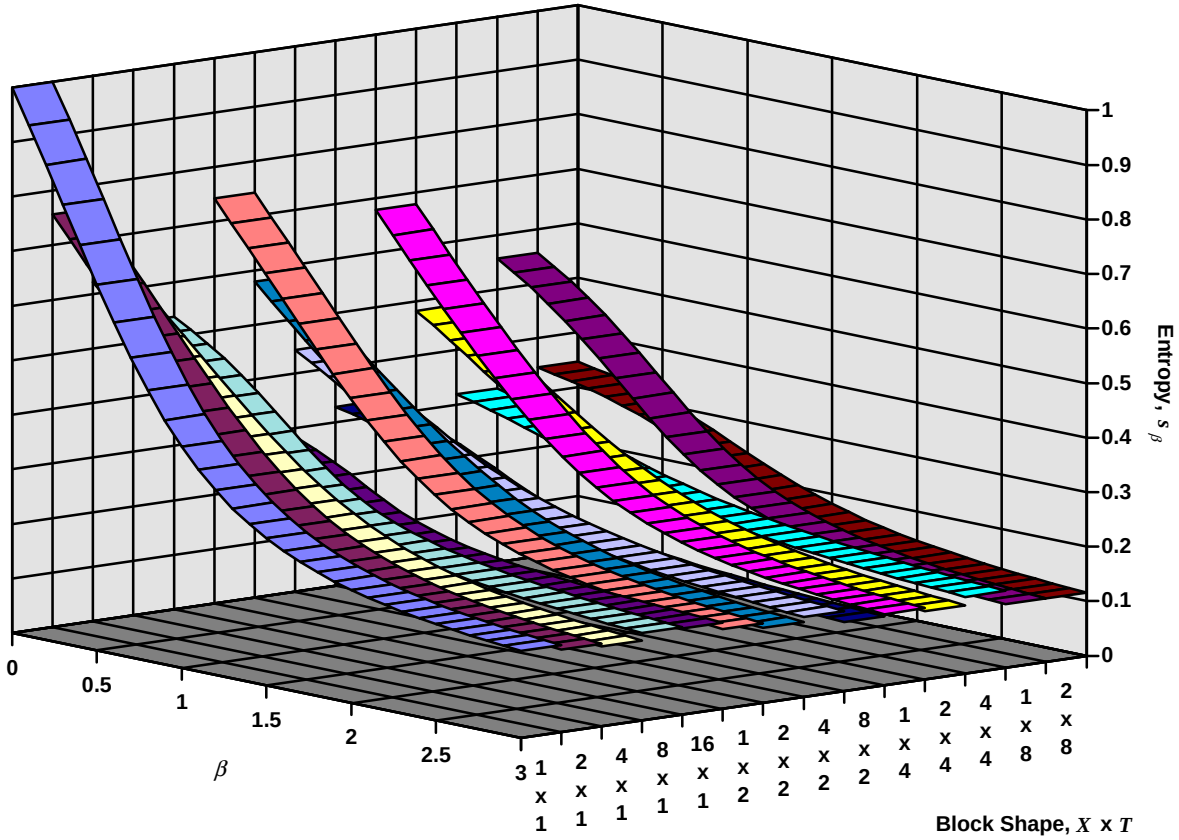

Figure 10. Experimental dependence of entropy $s_\beta(X,T)$ on block length X and duration T as a function of number of cells in 76,800 samples of a 256-cell CA with periodic boundary conditions and having 48 vehicles.

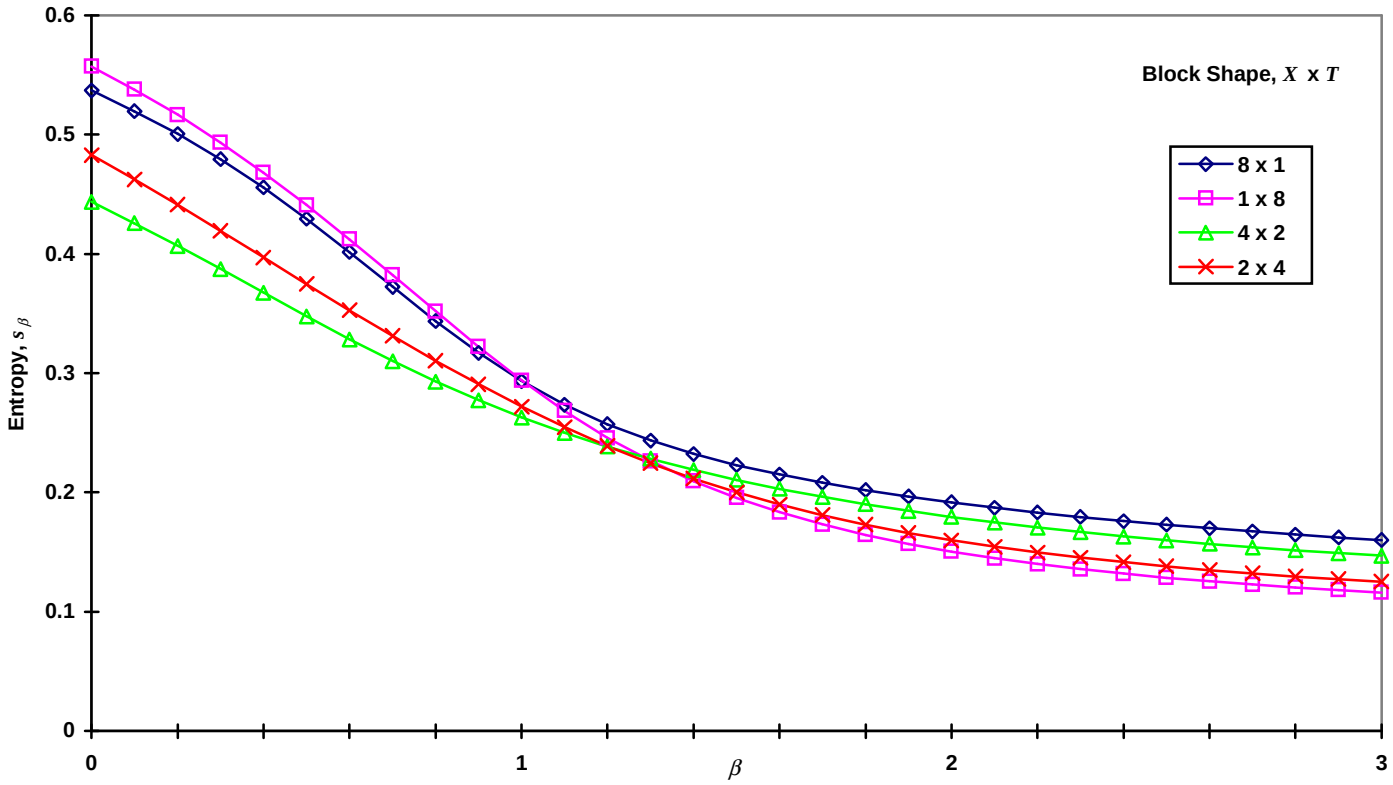

Figure 11. Experimental dependence of entropy $s_\beta(X,T)$ on block length X and duration T as a function of number of cells in 76,800 samples of a 256-cell CA with periodic boundary conditions and having 48 vehicles.

Dimension

So far, we have not been able to obtain a reliable value of the dimension

(17a) $$d_{\beta}^{X}(T) = \lim_{X \to \infty} s_{\beta}(X, T)$$

because of the difficulty of taking the limit experimentally.

Pattern Database

It is practical to build histograms of the states in a $X \times T$ block on CA lanes if T is not too large. The set entropy measurements from the numerical experiments provide an estimate of how many states might be seen and how much memory is required. Implementation would rely on efficient hash tables.

Such a “pattern database” would provide a detailed description of the dynamics in the CA, without involving the extensive disk storage required for collecting evolution/trajectory data.

Data Compression

The measure entropy estimates in the numerical experiments provide an indication of how much data compression might be possible when storing CA evolution/trajectory data.

Simple, low-overhead data compression schemes can be constructed using the idea of states in blocks.

Block Dynamics

It may be possible to speed up the CA computations by performing them on blocks rather than on individual vehicles: Instead of determining the behavior of each vehicle separately, treat vehicles in a block so that the dynamics are that of block transitions. This would require either Markov matrices of block transition probabilities or an approximate analytic representation of the process.

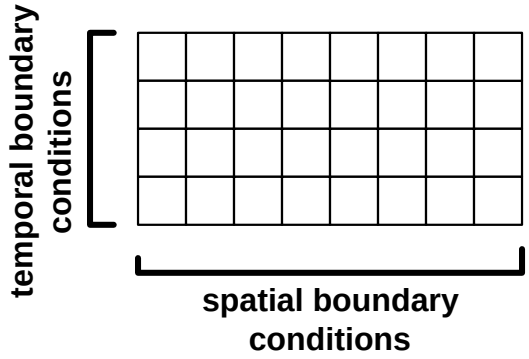

Entry/exit/parking cells would have to be treated specially. Also, vehicle identity does not necessarily have to be retained within a block.

Multiresolution Analysis

A *multiresolution analysis* of L^2 is a chain of subspaces $\{V_j : j \in \mathbf{Z}\}$ satisfying the following:

Containment: $V_j \subset V_{j-1} \subset L^2$ for all $j \in \mathbf{Z}$

Decrease: $\lim_{j \to \infty} V_j = 0$

Increase: $\lim_{j \to -\infty} V_j = L^2$

Dilation: $v(2t) \in V_{j-1}$ iff $v(t) \in V_j$

Generator: $\exists \phi \in V_0$ such that $\{\phi(t-k) : k \in \mathbf{Z}\}$ is a basis for V_0

[Wi 94]

Wavelets

From the *scaling function,* which obeys

(23) $$\phi(t) = \sqrt{2}\sum_{k\in\mathbf{Z}} h(k)\phi(2t-k) = \hat{H}\phi(t)\ ,$$

we can construct the *mother wavelet*

(24) $$\psi(t) = \sqrt{2}\sum_{k\in\mathbf{Z}} (-1)^k h(1-k)\phi(2t-k) = \hat{G}\phi(t)\ .$$

The mother wavelet is the generator for a basis in the *wavelet subspaces,*

(25) $$W_j = V_{j-1} - V_j\ ,$$

which provides a decomposition of L^2:

(26) $$L^2 = \sum_{j\in\mathbf{Z}} W_j$$

Wavelet Decomposition and Wavelet Packet Transform

Wavelets make possible scale-specific, localized decompositions of functions. A variety of scaling functions are available, and given a particular scaling function, many bases are possible.

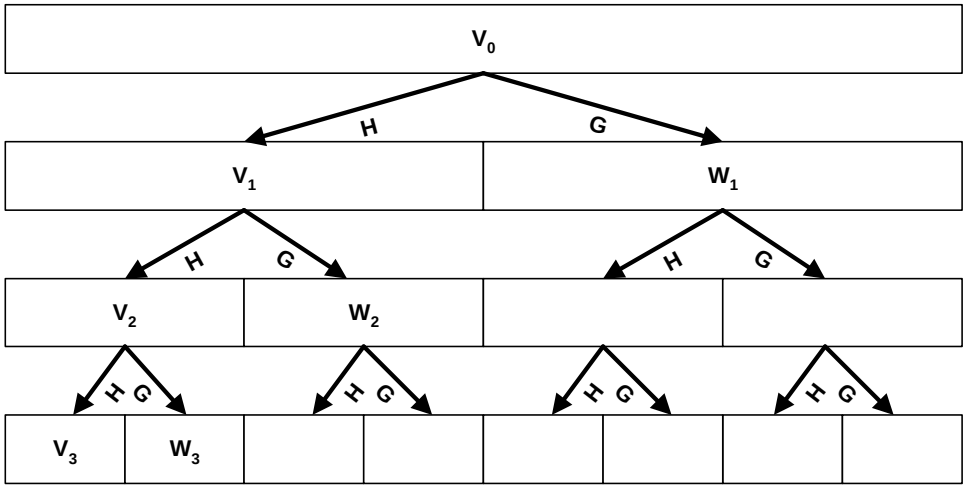

These provide a means for separating out emergent behavior at different scales in a traffic CA. The transform involves $O(n)$ additions and multiplications for n data points.

Choice of Scaling Function

Given a particular scaling function, the “best” basis can be chosen by minimizing the information required to describe functions of interest using the basis. Haar basis functions are especially useful for vehicle traffic.

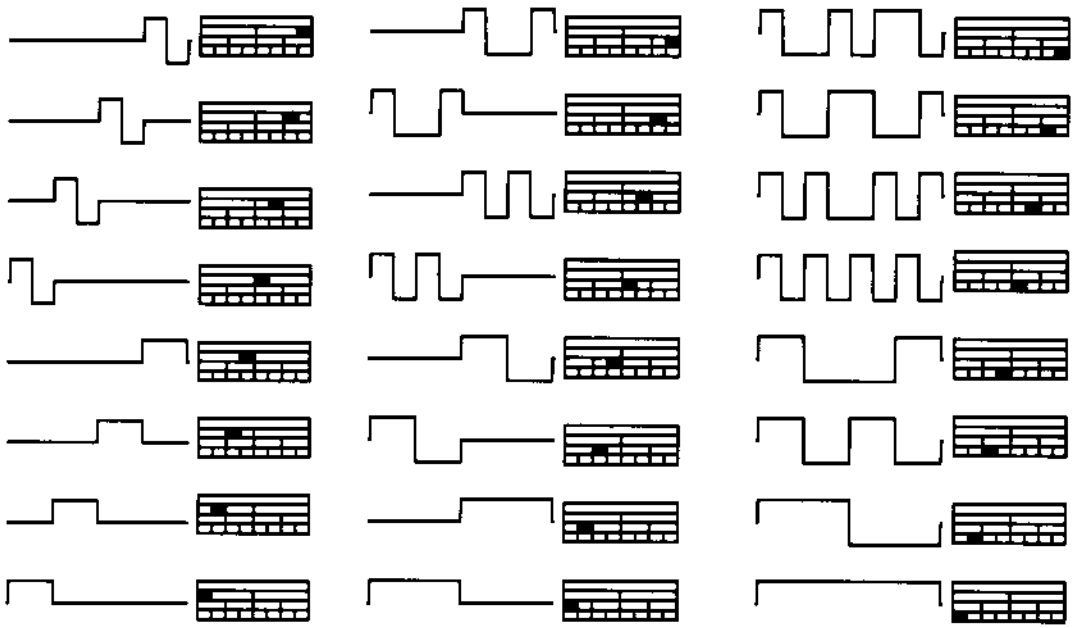

[Wi 94]

Scaling of Grid Cells

Instead of labeling the complete state of a group of cells, one can assign a label that aggregates the information in the group. For instance, groups of cells can be labeled by their number of vehicles and total velocity. This is similar to the current link box data collection in the CA.

These group functions do not necessarily have to preserve vehicle counts or velocities, but it is preferable that they do not bias averages. For example, each pair of cells can be combined into a new cell that has either zero or two vehicles an integer velocity—the states of such cells can be labeled just as single cells are. It would be interesting to understand how the CA output behaves under such as factor-of-two scaling.

The dynamics of cell groups can be derived from the driving behavior, or postulated *a priori*.

Other Scaling Behavior

Scaling behavior may also be present in observations of gap distributions, clusters, velocity distributions, correlation functions, etc.

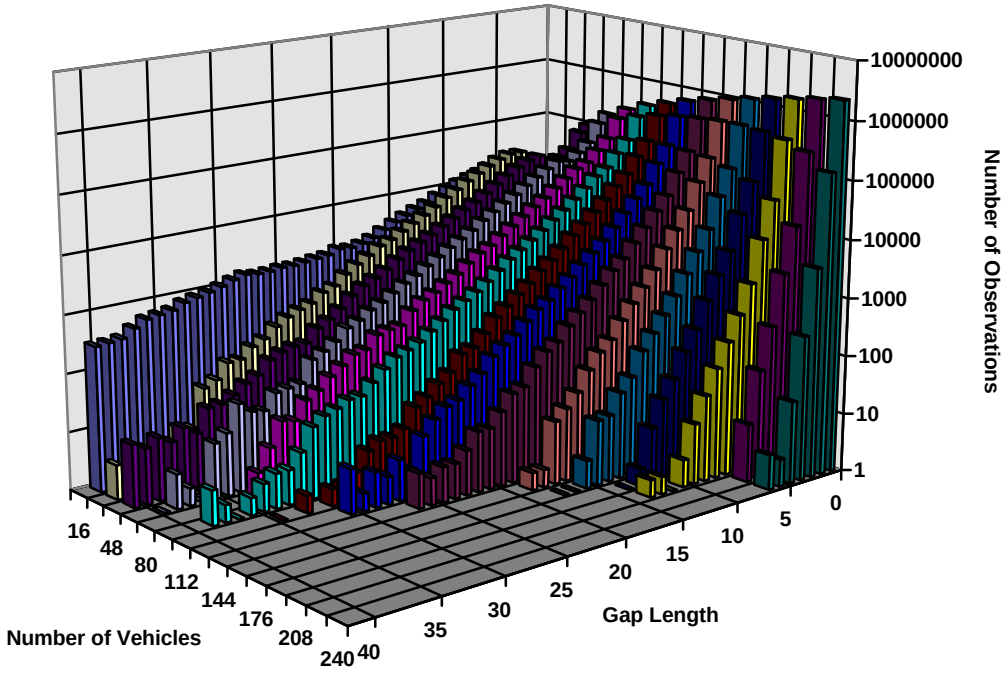

Figure 12. Experimental distribution of gap length frequency on number of vehicles in 10,000 time steps of a 256-cell CA.

Prospects

New types of data collection are possible, practical, and interesting.

The block/state formalism provides a means to look at patterns in the CA, measure information content, and perform data compression.

Multiresolution analysis using wavelets makes it possible to separate the CA behavior at a variety of space- and time-scales.

Analysis of other scaling behavior in the CA is possible.

It may be possible to speed up CA calculations using block dynamics or scaling laws.